NAVAL POSTGRADUATE SCHOOL

MONTEREY, CALIFORNIA

THESIS

WAVE CURRENT INTERACTIONS AND WAVE-BLOCKING PREDICTIONS USING NHWAVE MODEL

by

Kaitlyn E. Longley

March 2013

Thesis Advisor: Jamie Macmahan
Thesis Co-Advisor: Edward Thornton

THIS PAGE INTENTIONALLY LEFT BLANK

REPORT DOCUMENTATION PAGE			*Form Approved OMB No. 0704–0188*
Public reporting burden for this collection of information is estimated to average 1 hour per response, including the time for reviewing instruction, searching existing data sources, gathering and maintaining the data needed, and completing and reviewing the collection of information. Send comments regarding this burden estimate or any other aspect of this collection of information, including suggestions for reducing this burden, to Washington headquarters Services, Directorate for Information Operations and Reports, 1215 Jefferson Davis Highway, Suite 1204, Arlington, VA 22202–4302, and to the Office of Management and Budget, Paperwork Reduction Project (0704–0188) Washington DC 20503.			
1. AGENCY USE ONLY ***(Leave blank)***	**2. REPORT DATE** March 2013	**3. REPORT TYPE AND DATES COVERED** Master's Thesis	
4. TITLE AND SUBTITLE WAVE CURRENT INTERACTIONS AND WAVE-BLOCKING PREDICTIONS USING NHWAVE MODEL		**5. FUNDING NUMBERS**	
6. AUTHOR(S) Kaitlyn E. Longley			
7. PERFORMING ORGANIZATION NAME(S) AND ADDRESS(ES) Naval Postgraduate School Monterey, CA 93943–5000		**8. PERFORMING ORGANIZATION REPORT NUMBER**	
9. SPONSORING /MONITORING AGENCY NAME(S) AND ADDRESS(ES) N/A		**10. SPONSORING/MONITORING AGENCY REPORT NUMBER**	
11. SUPPLEMENTARY NOTES The views expressed in this thesis are those of the author and do not reflect the official policy or position of the Department of Defense or the U.S. Government. IRB Protocol number ____N/A____.			
12a. DISTRIBUTION / AVAILABILITY STATEMENT Approved for public release; distribution is unlimited		**12b. DISTRIBUTION CODE**	

13. ABSTRACT (maximum 200 words)

Wave blocking in river inlets is examined using the NHWAVE (Non-Hydrostatic Wave) model under development. Blocking flows at river inlets are a significant hazard to navigation. Refractive and shoaling effects contribute to the enhancement of wave field energy, causing instabilities and breaking, resulting in energy dissipation and transfer at the blocking point. The non-linearity of wave-current interactions and wave breaking makes the dynamics of blocking flows difficult to model. Current efforts to use wave-averaged models are insufficient to describe the complex dynamics that occur within one or two wavelengths of a blocking point. NHWAVE uses the non-hydrostatic, incompressible Navier-Stokes equations to model fully dispersive wave processes in the time domain. Monochromatic wave cases are explored and compared with lab experiments of energy dissipation due to wave breaking under conditions of strong opposing current, conducted in 2002 at the University of Delaware by A. Chawla and T. J. Kirby. The model was initially unable to resolve the boundary conditions necessary to model wave blocking in a tank domain. However, developments to the numerical scheme in NHWAVE have advanced its capability in this regard. Due to the difficulties of modeling the dynamics of wave blocking and the boundary conditions in a wave tank, only preliminary results were obtained. NHWAVE needs further development; it shows promise, however, to be able to predict wave reflection, blocking, and dissipation on a strong opposing current.

14. SUBJECT TERMS wave blocking, wave-current interactions, SWASH, NHWAVE			**15. NUMBER OF PAGES** 61
			16. PRICE CODE
17. SECURITY CLASSIFICATION OF REPORT Unclassified	**18. SECURITY CLASSIFICATION OF THIS PAGE** Unclassified	**19. SECURITY CLASSIFICATION OF ABSTRACT** Unclassified	**20. LIMITATION OF ABSTRACT** UU

NSN 7540–01–280–5500

Standard Form 298 (Rev. 2–89)
Prescribed by ANSI Std. 239–18

THIS PAGE INTENTIONALLY LEFT BLANK

Approved for public release; distribution is unlimited

WAVE CURRENT INTERACTIONS AND WAVE-BLOCKING PREDICTIONS USING NHWAVE MODEL

Kaitlyn E. Longley
Lieutenant, United States Navy
B.S., United States Naval Academy, 2004

Submitted in partial fulfillment of the
requirements for the degree of

MASTER OF SCIENCE IN METEOROLOGY AND PHYSICAL OCEANOGRAPHY

from the

NAVAL POSTGRADUATE SCHOOL
March 2013

Author: Kaitlyn E. Longley

Approved by: Jamie Macmahan
Thesis Advisor

Ed Thornton
Thesis Co-Advisor

Peter Chu
Chair, Department of Oceanography

THIS PAGE INTENTIONALLY LEFT BLANK

ABSTRACT

Wave blocking in river inlets is examined using the NHWAVE (Non-Hydrostatic Wave) model under development. Blocking flows at river inlets are a significant hazard to navigation. Refractive and shoaling effects contribute to the enhancement of wave field energy, causing instabilities and breaking, resulting in energy dissipation and transfer at the blocking point. The non-linearity of wave-current interactions and wave breaking makes the dynamics of blocking flows difficult to model. Current efforts to use wave-averaged models are insufficient to describe the complex dynamics that occur within one or two wavelengths of a blocking point. NHWAVE uses the non-hydrostatic, incompressible Navier-Stokes equations to model fully dispersive wave processes in the time domain. Monochromatic wave cases are explored and compared with lab experiments of energy dissipation due to wave breaking under conditions of strong opposing current, conducted in 2002 at the University of Delaware by A. Chawla and T. J. Kirby. The model was initially unable to resolve the boundary conditions necessary to model wave blocking in a tank domain. However, developments to the numerical scheme in NHWAVE have advanced its capability in this regard. Due to the difficulties of modeling the dynamics of wave blocking and the boundary conditions in a wave tank, only preliminary results were obtained. NHWAVE needs further development; it shows promise, however, to be able to predict wave reflection, blocking, and dissipation on a strong opposing current.

THIS PAGE INTENTIONALLY LEFT BLANK

TABLE OF CONTENTS

LIST OF FIGURES

THIS PAGE INTENTIONALLY LEFT BLANK

LIST OF ACRONYMS AND ABBREVIATIONS

NHWAVE	Non-Hydrostatic Wave
CK02	Chawla and Kirby 2002 Experimental Study
NLSW	Non-Linear Shallow Water Equations
RANS	Renold's Averaged Navier-Stokes Equations
VOF	Volume of Fluid
MAC	Marker and Cell
SPH	Smoothed Partical Hydrodynamics
SWASH	Simulating Waves till Shore
CFL	Courant-Fredrichs-Lewy
MPI	Message Passing Interface
ADV	Acoustic Doppler Velocimeter

THIS PAGE INTENTIONALLY LEFT BLANK

ACKNOWLEDGMENTS

This thesis would not have been possible without the guidance and the help of several individuals who in one way or another contributed to the preparation and completion of this study.

First and foremost, my utmost gratitude to Professor Fengyan Shi of the University of Delaware, who was there every step of the way as I hurdled all the obstacles in the completion this research work. Allowing me the opportunity to visit UDel and see the exciting work in both tank experiments and modeling efforts was above and beyond a thesis student's expectation. His help in the minute details of model coding were an invaluable resource. As often as I tried to break NHWAVE, he was there to help fix it.

To my advisor, Professor Jamie Macmahan, whose enthusiasm toward the development of his students is greatly appreciated. His dedication to new and exciting study in the nearshore region is contagious. My sincere thanks for allowing me the independence to develop my research, but always being there to guide me in the right direction.

Professor Emeritus Edward Thornton has been an inspiration to a new generation of nearshore scientists. His unfailing support as a mentor and teacher is a gift to NPS students. Above all, his encouragement, insightful comments, and difficult questions have shaped this thesis and my outlook on oceanography.

Last, but certainly not least, I extend a sincere thanks to my peers. Through the fun times and the tough, we've found a way to laugh. The support and encouragement we all share is something to be admired and cherished.

THIS PAGE INTENTIONALLY LEFT BLANK

I. INTRODUCTION

Wave fields propagating into regions of significant opposing flow, such as at the mouth of a tidal inlet, can be a significant hazard to navigation for mariners, affect the design of coastal structures, and alter the transport of sediment in the near shore region. As a wave field propagates into an opposing current, the group velocity reduces leading to an increase in wave height and decrease in wavelength. These waves can break causing energy dissipation, or the group velocity can go to zero in which case the wave field is blocked. If the current is not strong enough and the wave amplitude is relatively small, the waves can also be reflected from the blocking point. Energy transfers in blocking flow cause the wave environment to become very rough and difficulties in navigating and transiting these inlet areas are common.

A. WAVE BLOCKING THEORY

The basis of previous research on small-scale wave-current interactions is the Doppler-shifted dispersion relation for waves moving on uniform currents (Perigrine 1976). In the case of a wave field opposing a tidal current, the time and length scales for the tidal current flow are much larger than the wave period and wavelength. This allows kinematic properties of plane waves to be applied on uniform currents. By applying a depth uniform current **U** and using a reference frame that is moving with the current, the equations and solutions for water-wave movement are the same as for no current (Jonsson 1990). Previous study of waves moving on a vertically sheared but weak current showed that by using the small parameter ε=U/c, where c is the wave phase speed, through O(ε)

$$(\omega - kU\cos\alpha)^2 = gk\tanh(kh) = \sigma^2 \tag{1}$$

where ω and k are the fixed reference frame radian frequency and wave number, and σ is the intrinsic frequency defined by linear theory (Kirby and Chen 1989). The still water depth is *h* and α is the angle between wave propagation and the underlying current. This is identical to the dispersion relation for arbitrary water depth using the intrinsic

frequency ω-**k•U**. Defining ω as wave frequency in a reference frame moving with the current, the wave phase speed in both frames of reference is related by

$$\frac{\omega}{|k|} = \frac{\sigma}{|k|} + |U|\cos\alpha \tag{2}$$

or

$$\omega - k \cdot U = \sigma \tag{3}$$

where wave number, k, remains unchanged in the two reference frames. Application of σ is dependent on the wave theory used.

The kinematic wave blocking condition is described using the Doppler-shifted dispersion relation for waves and is obtained by assuming depth uniform currents, Equation (3), along with an expression for ω. Differentiating with respect to k and setting the group velocity to zero gives

$$\frac{\partial \sigma}{\partial k} = -U \tag{4}$$

where

$$U \equiv |U|\cos\alpha \tag{5}$$

Due to the cosα term, blocking only occurs for α between 90° and 270° (Chawla and Kirby 2002).

The graphical solution of the Doppler-shifted dispersion relation, Equation (3), shows the limits of different wave-blocking scenarios to be addressed in this paper, (Figure 1). Using linear wave theory, Equation (1) becomes $\sigma = \sqrt{gk\tanh kh}$, and is plotted as a blue curve for the case of currents directly opposing the wave field, α=180°. In Figure (1a), Equation (3) is computed with a constant current speed, U_1 for different ω values and plotted as a green, red, and cyan line (ω_1, ω_2, and ω_3). For increasing frequency and a constant current, U, the solution evolves from wave-current interactions, to a blocked wave field. The ω_1 line is a solution for waves below the blocking frequency for the given current. These waves will have interaction with the current, but will not be blocked. Where $\omega - k \cdot U = \sigma$ becomes tangent to Equation (1) at point **A**, defines the

blocking solution. This Doppler-shifted solution represents the frequency at which the given current will block the wave field. Waves above this curve have no solution; this is indicated by ω_3 in which all waves will be blocked.

The blocking scenario is categorized in Figure (1b) where the dispersion relation is solved at a particular frequency, ω_2. The horizontal line represents a wave only scenario with U=0. Solutions below this line, in the dotted area, will have no current interactions. This is the case for solutions from point **A** to point **B**. From point **B** to **C**, in the presence of an opposing current, the wave number will increase and the wavelength will become shorter. Here, the solutions are shown in the vertically lined section. As k increases further and the group velocity decreases, the complete blocking scenario is reached and is represented by point **C**. There is no solution for waves interacting with stronger currents above the ω_2 line and therefore the solution never increases over this line for a blocking current. For current smaller than the wave blocking current but with higher k, there is a solution in the wiggly line section. In this case, while the waves are moving opposite the flow, the wave energy travels with the current, opposite the wave motion. The solution represents reflection and partial wave blocking (Chawla, 1999).

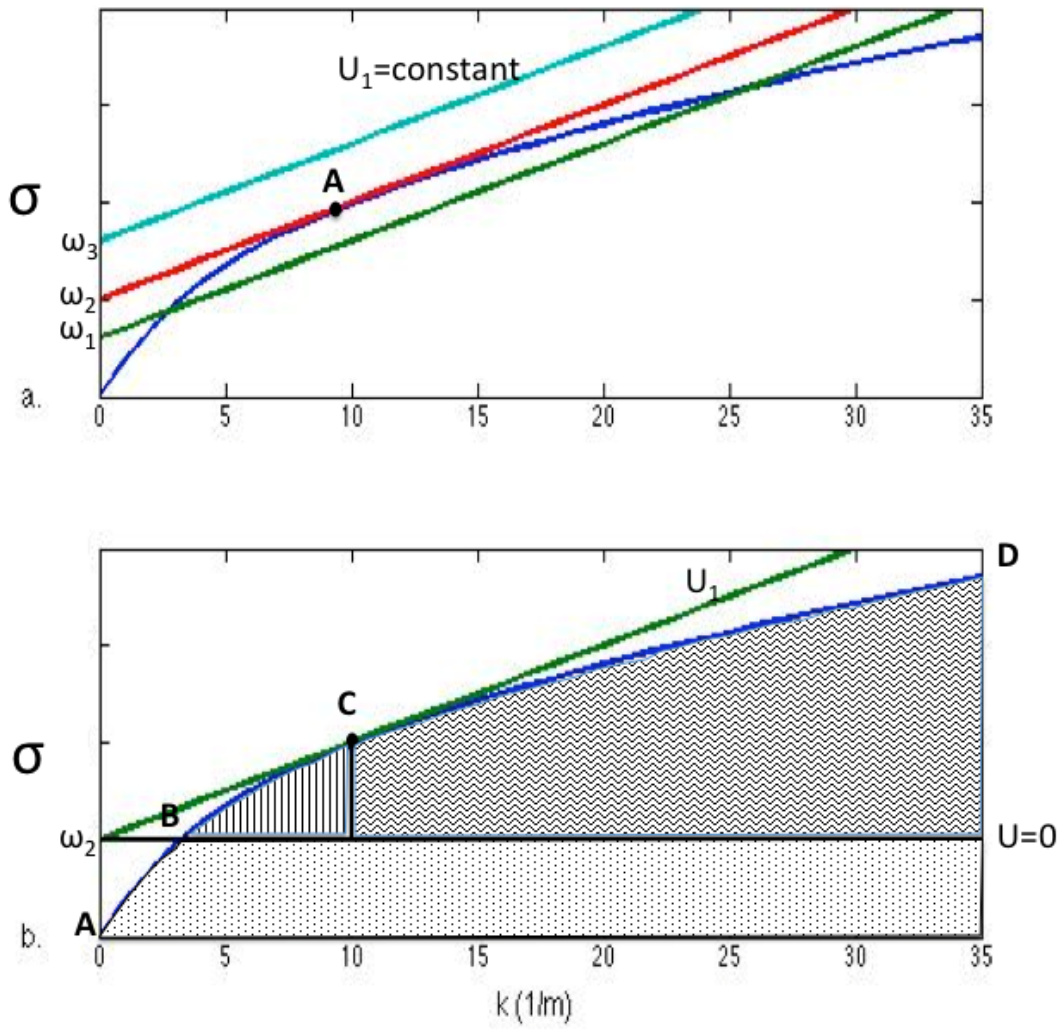

Figure 1. Graphical solution to the dispersion relation. a) Solution for constant current and different frequencies ω_1, ω_2, and ω_3. b) Solution for increasing current, dots=wave only, lines=wave-current interaction, wiggly lines=wave-current interactions with some reflection

B. BASIS FOR STUDY

The Office of Naval Research has directed research initiatives to study the complex wave-current dynamics in the nearshore region. As the Navy moves further inshore and upstream, these conditions at river inlets become more important to understand. This effort is focused on developing a model that can handle the complex

dynamics and boundary conditions involved in modeling a tank domain with both waves and currents so that future application to the field is possible.

Most previous studies and theoretical analyses on wave blocking have been limited to linear wave theory. Due to the sharp steepening of waves just prior to the blocking point, this approach is only valid for small amplitude waves. In locations such as a river inlet, where wave heights can be great, an approach that can model the non-linear effects is needed.

1. Motivation

Wave-current interactions are an important consideration in coastal oceanography. Non-linear interactions can cause significant effects to mass transport, large amplitude wave crests can cause damage to coastal structures, and the turbulence induced by the kinematics can be dangerous for maritime vessels. Modeling these effects to predict the dynamic conditions in areas of opposing flow and wave-blocking is of great importance and is difficult. Despite recent studies in non-linear wave-current interactions, there is still a limited understanding of how energy is transferred or dissipated at wave blocking locations.

Field measurements at river inlets, where a strong ebb tidal jet meets an opposing wave field inducing significant wave-current interaction and wave-blocking, are becoming more common with improvements in field observation techniques and instruments. Simulating these conditions in a model poses issues of scaling and boundary conditions that are not present in field data. Simulating a tank condition in a model domain further removes the dynamics from the environmental truth but is necessary to study individual wave components and improve understanding of energy transfers through blocking regions.

Understanding wave blocking with NHWAVE allows for potentially better parameterization with more robust wave-averaged models that run faster. Currently those models under predict wave heights and breaking by about one half. This is due to the non-linear effects occurring at distances on the order of a wavelength, this causes wave solutions in wave-averaged models to fail.

A model of the wave-current interactions at an inlet can potentially describe the fully non-linear processes in wave blocking. A number of difficulties are associated with numerical implementations in modeling, which will be described in this research. This study will review some of the contemporary attempts to model and predict the physics of wave blocking and discuss the development of one model in particular.

2. Objective

In the Chawla and Kirby (2002) experimental study, hereafter referred to as CK02, monochromatic and random wave fields were created with an opposing current in a wave flume. A conservation of wave action numerical model was used to describe waves on an opposing current. A simple probabilistic bore model was used to describe dissipation by wave breaking to replicate the lab data. While good correlations with laboratory data were obtained in this simplified model, extension to a more complex model that can handle dynamics in the wave-blocking region in the time domain is attempted here.

The objective of this research is to develop the NHWAVE model (described in future sections) to predict wave-current interactions and blocking compared with extensive laboratory data described in CK02. Of particular interest is the amplitude envelope of monochromatic waves in cases varying from complete blocking and reflection, to total wave transmission through the blocking point. Energy transfers and dissipation in larger amplitude breaking wave cases will also be explored in the model. In the following, data from the tank experiment is used to develop a model in a refractive, monochromatic wave setting. NHWAVE has been modified to characterize wave-current interactions in a new and innovative way, showing its potential in this modeling environment, and adding relevance to more general modeling of wave blocking at river inlets.

II. THEORETICAL BACKGROUND

A. INTRODUCTION

Previous studies of wave-current interactions have been limited to linear wave theory. However, when the opposing current is strong enough, waves become blocked, and linear theory breaks down at the blocking point. Both refractive and shoaling effects contribute to the enhancement of energy, causing instabilities and breaking that result in energy dissipation and transfer at the blocking point. The non-linearity of wave-current interactions makes the dynamics of blocking flows difficult to model.

B. PREVIOUS MODEL APPROACHES

1. Boussinesq Models

Non-linear Boussinesq-type wave models have been used to describe the refraction, diffraction, shoaling, and breaking of wave fields in the coastal region. The original equations by Boussinesq (1872), describes water waves in incompressible, inviscid fluid and non-rotating flow and are based on combining the horizontal momentum flux and the continuity equations and retaining terms $\left(\frac{a}{h(kh)^2}\right) = O(1)$, the Ursell Number, where a is amplitude,

$$\frac{\partial^2 \eta}{\partial t^2} - gh\frac{\partial^2 \eta}{\partial x^2} - gh\frac{\partial^2}{\partial x^2}\left(\frac{3}{2}\frac{\eta^2}{h} + \frac{1}{3}h^2\frac{\partial^2 \eta}{\partial x^2}\right) = 0 \tag{6}$$

η is the free surface elevation, g is the gravitational acceleration, and t and x are time and horizontal location. Models based on this theory with improved non-linearity and dispersion characteristics by including higher order terms have been well tested and are efficient models of wave propagation. The non-linear aspects of the improved models allow the amplitude dispersion and energy transfer effects in wave blocking scenarios to be well represented. Conversely, for short waves, wave dispersion properties are not well predicted and this deviation only increases with increasing wave number. The governing

equations do not include dissipation due to wave breaking, and thus, become invalid under any breaking conditions. Attempts to include turbulent mixing and dissipation caused by breaking in these models have used artificial eddy viscosity terms (Heitner and Housner 1970, Tau 1983, Zelt 1991, and Kennedy et al. 2000 amongst others). This approach is useful for weakly non-linear waves, with longer wavelengths. However, this is not the case in wave-blocking scenarios, and therefore these methods are not sufficient to model wave-breaking on an opposing current and the turbulence that occurs at wave-blocking points.

2. Non-linear Shallow Water Equations (NLSW)

The non-linear shallow water equations assume a hydrostatic pressure distribution that is violated at the point of wave-breaking. In basic form

$$\begin{aligned} \frac{dD}{dt} + u\frac{dD}{dx} + D\frac{du}{dx} &= 0 \\ \frac{du}{dt} + u\frac{dx}{du} + g\frac{dD}{dx} &= 0 \end{aligned} \tag{7}$$

where u is the horizontal current velocity and $D = \eta + h$ is the water depth.

Traditionally, the effect of non-hydrostatic pressure can be modeled using the Bousinesque-type approximation and adding higher order terms to the NLSW equations. The NLSW equations are then extended with the addition of the vertical motion equation, a deviation from hydrostatic pressure, making them equivalent to the incompressible Navier-Stokes equation. In this approach, as with previous modeling techniques, there is difficulty in simulating the free surface that inhibits accurate prediction of wave-current interactions at blocking points.

3. Renolds Averaged Navier-Stokes Equations (RANS)

These efforts led to solving the Reynolds averaged Navier-Stokes equations with simultaneous computation of the vertical structure and horizontal variations,

$$\rho\overline{u}_j\frac{\partial\overline{u}_i}{\partial x_j}=\rho\overline{f}_i+\frac{\partial}{\partial x_j}\left[-\overline{p}\delta_{ij}+\mu\left(\frac{\partial\overline{u}_i}{\partial x_j}+\frac{\partial\overline{u}_j}{\partial x_i}\right)-\rho\overline{u_i'u_j'}\right]\qquad\begin{matrix}i=1,2,3\\ j=1,2,3\end{matrix}\tag{8}$$

where f is representative of external forces and the over-bar indicates time averaging. The instantaneous velocity and pressure terms are decomposed into a constant and a fluctuating component that are time averaged on the scale of the wave period. In both the Boussinesq and NLSW equation methods, uniform pressure and velocity distributions are assumed. Also, the RANS method does not employ the simple turbulence parameterization as in previous methods.

4. Free Surface Treatment

Of importance in all modeling techniques is the treatment of the free surface and obeying the balance of pressure forces across the boundary. Methods include the Volume-of-Fluid (VOF), Marker and Cell (MAC) and Smoothed Partical Hydrodynamics (SPH) methods (Zijlema and Stelling 2011). Drawbacks to these model techniques include coarse resolution on the interwave scale, inaccurate velocity computations where the pressure boundary condition is not met, and computational inefficiency. Because of these inadequacies, it may not be possible to accurately predict the onset of wave breaking and energy transfers that occur at wave-blocking river inlets.

The difficulties in modeling the pressure boundary condition necessitate non-hydrostatic approximations at the free surface to achieve the pressure balance at the boundary. Stelling and Zijlema (2003) used a Keller-box staggered grid, allowing pressures to be defined at the vertical cell faces rather than cell centers. This pressure boundary simplification and staggered grid in the vertical direction allow for non-hydrostatic approximations to be used at the surface, enabling wave propagation, turbulence, and solute transport calculations with fewer layers and a better representation of linear dispersion effects than previous models.

While the above approximations allow for the use of a non-hydrostatic pressure surface condition, models of turbulent conditions, such as wave breaking in the surf zone and run-up in the swash region, must be adequately modeled for shock propagation (Zijlema and Stelling 2008). This is accomplished by applying the Godunov-type approach for shock capturing and discontinuous flow. These schemes allow wave breaking to be calculated through a numerical approach rather than being prescribed in the modeling process (Ma et al. 2012).

III. MODEL DEVELOPMENT

A. INTRODUCTION

Two models were recently developed that use the non-hydrostatic Navier-Stokes equations in conservative form to model fully dispersive wave processes, NHWAVE (Non-Hydrostatic Wave Model) (Ma et al. 2012) and SWASH (Simulating Waves till Shore) (Zijlema et al. 2011). To study the complex wave-current interactions at blocking locations, an effort was begun to look at laboratory data and attempt to replicate it in a model environment so that future application to field data would be possible.

Initially, the SWASH model was tested to replicate the tank experiment data. SWASH is an open source code model simulating non-hydrostatic, free-surface, rotational flows in multiple dimensions. It is useful in predicting transformations of surface waves and rapidly varied shallow-water flows in coastal waters. It implements nonlinear shallow water equations and generally describes the complex changes due to rapidly changing parameters in a shallow water environment (Zijlema et al., 2011). This model has been through numerous benchmark tests and handles nearshore dynamics very well. The availability of implementation manuals, and vast examples of model use made independent work with the model possible. Ideally, this model would be able to handle the dynamics of the CK02 experiment.

Initial test cases with the SWASH model looked promising. The first steps were to define a wave tank with a false wall to replicate a river inlet and induce a wave field with an opposing current. SWASH has a user-friendly interface and the process was relatively simple. Model runs with a monochromatic wave field imposed at the boundary were consistent with expected linear theory. Separate tests to determine the current input as a mass flux at the boundary were also successful. However, it was not possible to include both dynamic inputs in the model. The boundary inputs of the model could handle a wave field or a current, but not both imposed over each other at the same location. After repeated attempts to correct the problem through the code and different inputs, it became apparent that there was no further way forward and help from the

developers was needed. Discussion about the boundary condition issue was initiated with model developers; however, this was an issue that would not easily be resolved and other options needed to be explored.

Open communication with peers at the University of Delaware in the Coastal Engineering Department facilitated discussion of the newly published model NHWAVE (Non-Hydrostatic Wave). Being able to consult with the developers of the model on a regular basis was of great importance. The model was published in May of 2012 and has undergone numerous benchmark tests. Contrary to SWASH, however, its main focus was on the prediction of Tsunamis and application to greater ocean depths than SWASH. These models differ primarily in their numerical approach to non-linear ocean processes. NHWAVE is developed for wave blocking in this research and described in the following.

B. NON-HYDROSTATIC WAVE MODEL (NHWAVE)

The NHWAVE model uses the σ_z coordinate system for both surface and terrain features as developed by Phillips (1957). The σ_z coordinate is defined as

$$\sigma_z = \frac{(z+h)}{D} \tag{9}$$

where D is the total depth (h+η) and z is measured positive upwards from the still water level. The coordinate transformation maps the bottom and surface to constant boundaries of a strip of unit thickness.

1. Governing Equations

Using the conservative Boussinesq equations in general form

$$\frac{\partial \Psi}{\partial t} + \nabla \cdot \Theta(\Psi) = S \tag{10}$$

Ψ is the vector for conserved variables and Θ(Ψ) is the numerical flux vector function.

$$\Psi = \begin{pmatrix} D \\ Du \\ Dv \\ Dw \end{pmatrix} \tag{11}$$

$$\Theta = \begin{pmatrix} Du\mathrm{i} + Dv\mathrm{j} + \omega\mathrm{k} \\ (Duu + \frac{1}{2}gD^2)\mathrm{i} + Duv\mathrm{j} + u\omega\mathrm{k} \\ Duv\mathrm{i} + (Dvv + \frac{1}{2}gD^2)\mathrm{j} + v\omega\mathrm{k} \\ Duw\mathrm{i} + Dvw\mathrm{j} + w\omega\mathrm{k} \end{pmatrix} \tag{12}$$

where (u,v) are velocity components in (x,y) and w is the vertical velocity in the σ_z coordinate system. The source term $\mathbf{S}$, is composed of three components, bottom slope $\mathbf{S}_h$, pressure gradient $\mathbf{S}_p$, and turbulent mixing $\mathbf{S}_\tau$.

$$\mathbf{S}_h = \begin{pmatrix} gD\dfrac{\partial h}{\partial x} \\ gD\dfrac{\partial h}{\partial y} \\ 0 \end{pmatrix} \quad \mathbf{S}_p = \begin{pmatrix} -\dfrac{D}{\rho}\left(\dfrac{dp}{dx} + \dfrac{dp}{d\sigma}\dfrac{d\sigma}{dx^*}\right) \\ -\dfrac{D}{\rho}\left(\dfrac{dp}{dy} + \dfrac{dp}{d\sigma}\dfrac{d\sigma}{dy^*}\right) \\ -\dfrac{1}{\rho}\dfrac{dp}{\partial\sigma} \end{pmatrix} \quad \mathbf{S}_\tau = \begin{pmatrix} D\mathbf{S}_{\tau_x} \\ D\mathbf{S}_{\tau_y} \\ D\mathbf{S}_{\tau_z} \end{pmatrix} \tag{13}$$

here, p is dynamic pressure only. The k-ε closure model is used to calculate the turbulent diffusion terms $\mathbf{S}_{\tau_x}$, $\mathbf{S}_{\tau_y}$, $\mathbf{S}_{\tau_z}$. In NHWAVE, the free surface governing equation can be written as

$$\frac{dD}{dt} + \frac{d}{dx}\left(D\int_0^1 u\, d\sigma_z\right) + \frac{d}{dy}\left(D\int_0^1 v\, d\sigma_z\right) = 0 \tag{14}$$

The dynamic pressure in the source terms is calculated by solving the Poisson equation in (x, y, σ_z) coordinate system. Further details of the calculation techniques are found in Ma et al (2012).

2. Numerical Scheme

Finite-volume and finite difference methods are used for special discretization. It is done in two steps, first using a reconstruction technique to compute values at cell interfaces, and second using a Reimann solver for numerical fluxes at the interface location. A central difference scheme is used for all source terms, **S**. NHWAVE uses a second-order Strong-Stability-Preserving (SSP) Runge-Kutta scheme for non-linear discretization

$$\begin{aligned} \Psi^{(1)} &= \Psi^{n} + \Delta t\left(-\nabla\cdot\Theta\left(\Psi^{n}\right)+S^{(1)}\right) \\ \Psi^{n+1} &= \frac{1}{2}\Psi^{n} + \frac{1}{2}\left[\Psi^{1} + \Delta t\left(-\nabla\cdot\Theta\left(\Psi^{1}\right)+S^{(n+1)}\right)\right] \end{aligned} \tag{15}$$

Within the above scheme, a two-step projection method splitting the time integration into hydrostatic and non-hydrostatic steps is used. An adaptive time step is used following the Courant-Friedrichs-Lewy (CFL) criterion. NHWAVE is run parallel using the domain decomposition technique. Non-blocking data communication between processors is done using the Message-Passing-Interface (MPI) when not in serial mode (Shi et al. 2012).

Computationally, a staggered grid approach is used defining velocities at cell centers and pressure at the vertical facing wall similar to the Keller-Box scheme. This allows accurate treatment of the pressure boundary condition at the surface. NHWAVE is capable of simulating wave refraction, diffraction, shoaling, breaking, landslide tsunami generation, and alongshore current. It can predict surface wave processes using few vertical layers with good accuracy as seen in benchmark tests (Tehranirad et al. 2012). Wave breaking and associated energy dissipation are also reasonably predicted by the model. Additional details of the development and testing of NHWAVE are found in Ma et al. (2012).

C. INITIAL MODEL TESTING

There are limitations inherent to ocean modeling and numerical code. While modeling of the physical processes has become computationally simpler with

developments to wave theory, any computer simulation will have difficulty in modeling all variables and especially boundary conditions.

> There is a world of difference between the character of the fundamental laws, on the one hand, and the nature of the computations required to breathe life into them, on the other. Berlinski (1996)

The current study was conducted through several iterations of the NHWAVE code. Both modifications to the source code, compilers, and the executable files were needed to model the wave-current interactions in a tank. NHWAVE continues to be under development and shows promise for future modeling efforts.

1. Wave Maker and Numerical Dissipation

Many of the issues with boundary conditions came as a result of trying to have a boundary that would produce a wave field, and also have a constant current flow. This study facilitated the creation of an internal wave maker. The wave maker is rather simple in principle in that it requires an amplitude, period, and depth input parameter. It then creates a wave field from within the tank boundaries with propagation in both the positive and negative x direction. By having a wave source contained within the boundary, the issue of dual dynamic conditions at the east and west boundaries was solved. However, the simplistic wave maker did not produce waves at the exact amplitude as the input, therefore adjustments to initial conditions were needed.

Initial tests of the model with waves only in the tank were conducted with a 0.1 m resolution in the x and y directions. The wave maker in the initial test introduced a wave field of 0.03 m amplitude and 1.2 s period. At this resolution, the internal linear wave maker is unable to produce a constant amplitude wave. Issues of numerical dissipation, seen in model data, caused amplitude damping that does not support wave theory (Figure 2). Amplitude damping occurred within 10 m of the wave maker in both a square tank, and the test tank with the false wall simulating an inlet at this resolution.

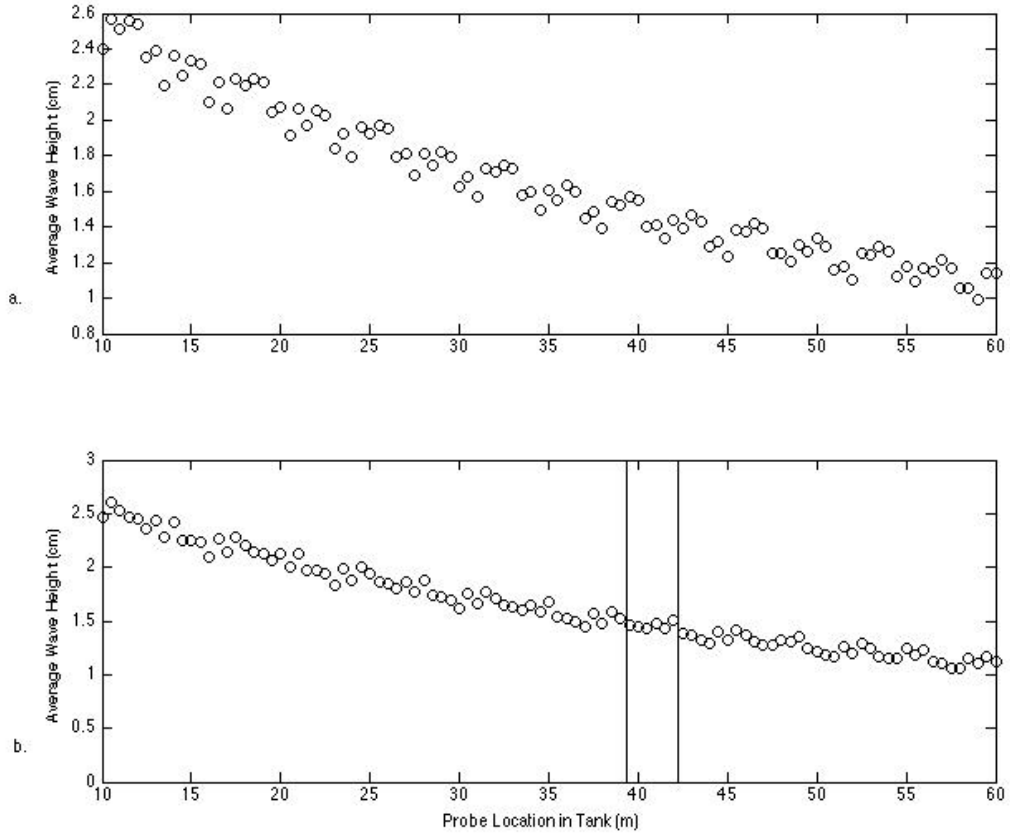

Figure 2. Wave height distribution through the tank at low resolution (0.1m) a.) Square tank. b.) Tank with false inlet wall. Vertical lines indicate first narrowing wall of the tank domain.

By increasing the resolution to 0.025 in the x direction and 0.05 in the y-direction the wave maker was able to produce steady waves that maintained amplitude with minimal damping through a square tank as seen in the wave height plotted through the model tank (Figure 3, blue line). However, amplitude damping was still present in the tank with the inlet wall (red line) as a result of a boundary condition issue to be described hereafter. Each case shows a consistent wave through the wide area of the tank; however, the red profile begins to dampen considerably upon reaching the inlet wall at 39.4 m.

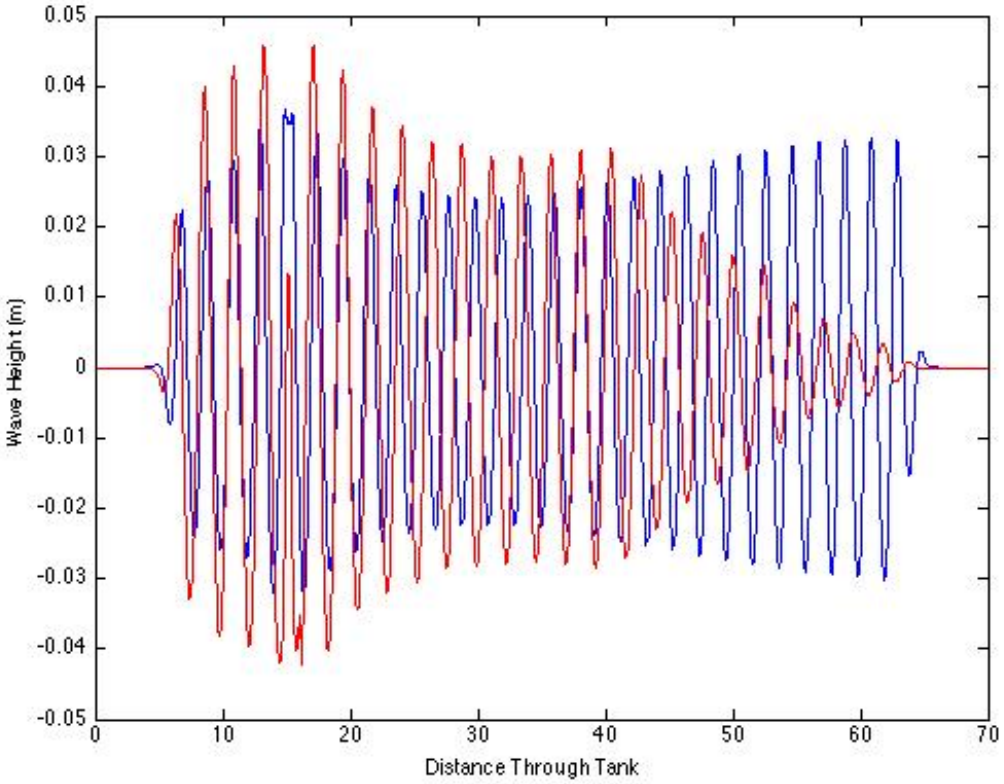

Figure 3. Wave height at high resolution for waves in a square tank with no current (blue), and waves in inlet tank, no current (red).

Numerical dissipation is caused by a numerical approximation of the partial differential equations assuming the theoretical equations are exact. For example, using a first order finite differencing scheme will truncate equations at the second order (dx^2). The truncated terms may be diffusive or dispersive. In this model, the terms are diffusive. NHWAVE uses a numerical approximation to the partial differential equations governing the internal wave maker in the tank. This process causes a dissipation of the wave down the tank that is a result of the numerics of the model rather than an actual physical process. In the model results, the wave maker showed amplitude damping throughout the tank that improved with increasing the horizontal resolution.

2. Boundary Conditions

In order to model the CK02 tank, great care was taken in developing the NHWAVE boundary conditions as mentioned previously. Having an internal wave maker was beneficial in simplifying the boundary inputs, however, other issues arose. Because the waves were created inside the domain, waves propagate in both directions and need to be dissipated at the boundaries to negate reflection from the east and west walls. Absorption of mass flux and energy at the boundary is also a concern for the current imposed in the domain. If the current is allowed to reflect off the boundaries, oscillations in the tank will form and create issues in the data.

Sponge layers on either side of the tank were created to dissipate wave energy and mass flux from the current. Throughout the modeling process modifications to the source code, to include dimension and decay coefficients, were needed in order to negate as much reflection from the tank "walls" as possible. By creating a low-pass filter imbedded in the sponge layers, oscillations and reflections were decreased to almost zero. The filter allows the current to pass through at a constant speed while filtering out any wave action. Wave energy is absorbed into the sponge layers at the east and west boundaries (Figure 4). Development of this aspect of the model is crucial to future iterations and uses of the model in experimental tank applications.

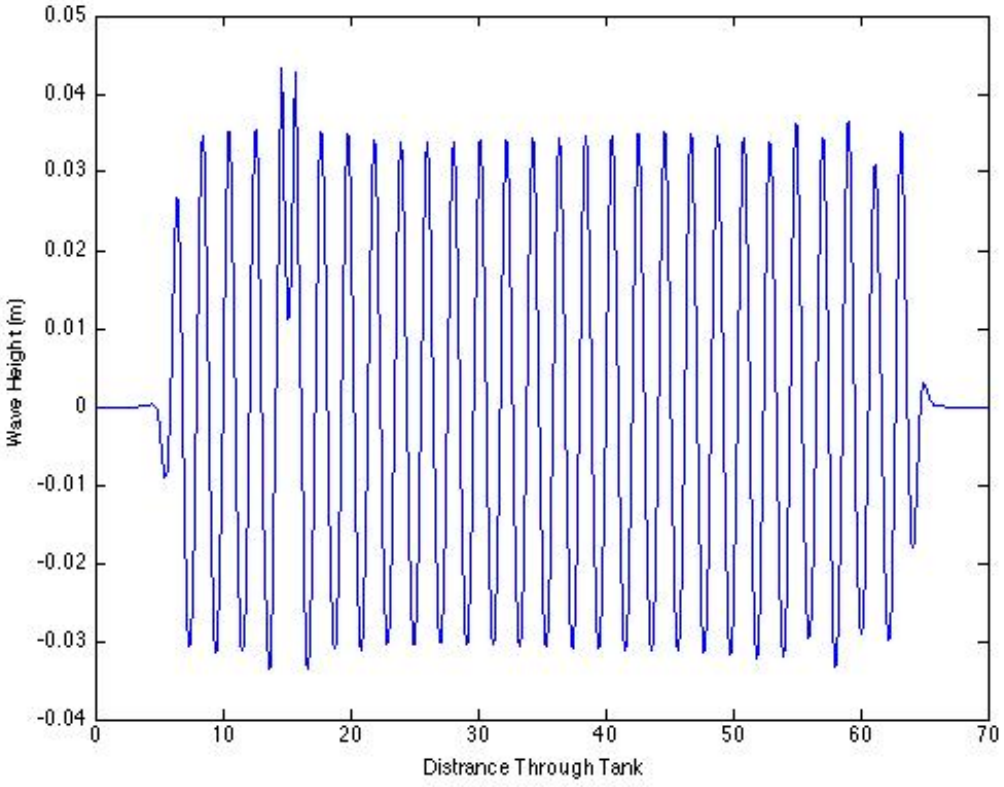

Figure 4. Low pass filtered sponge layers showing wave dissipation in the sponge layer with a .03 m 1.2 s wave, no reflection. Sponge layers are? 7 m wide.

No-slip boundaries were used on the north and south walls of the tank. This was done to reduce any change in current velocities or the wave field in the cross-tank dimension. Also, the bottom was defined as frictionless to maintain the constant vertical distribution of current assumption. The vertical and cross-tank distribution of current for the test cases shows little variability (Figure 5). This allows one-dimensional theories to be applied to the CK02 and model results.

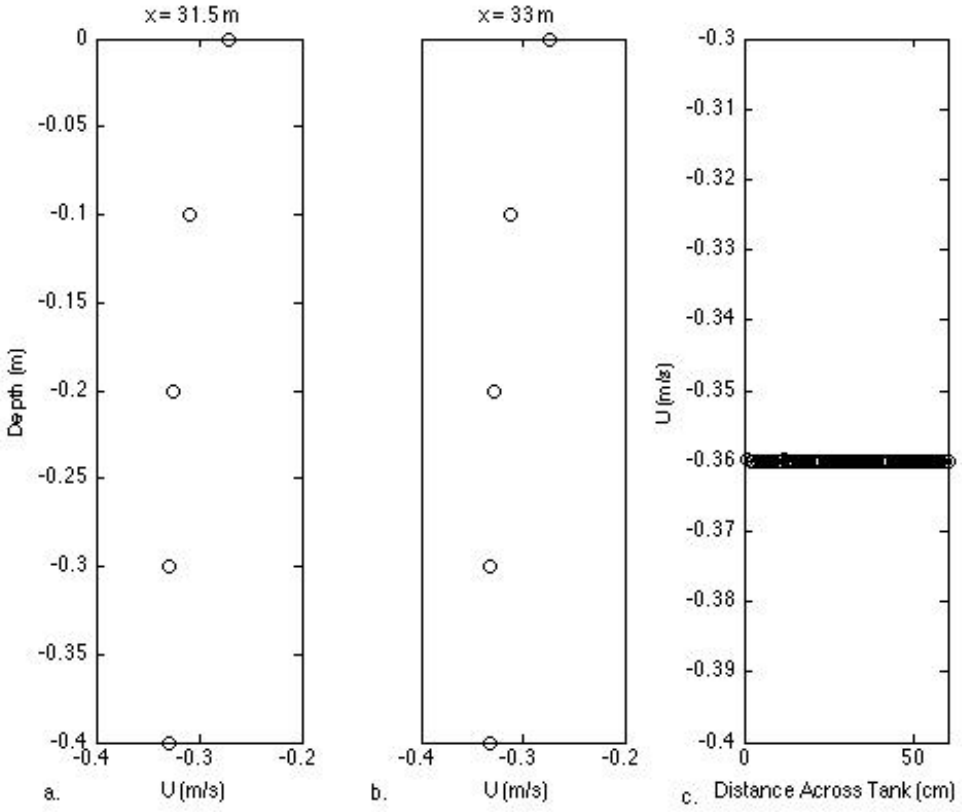

Figure 5. Vertical current distribution at a) 31.5 m and b) 33 m. c) Horizontal distribution across the tank at location 25 m.

3. Computational Efficiency

NHWAVE is set up to run in either parallel mode, using the message-passing interface (MPI), or in serial mode where a single node of computing is used. For this study, the high-powered computers in the Mills cluster at the University of Delaware were accessed to run the model. The model was programmed in Linux and Fortran. Due to nodal structure, computational efficiency was greatly increased by running in parallel mode. This was especially evident as grid resolution in the model was increased. Due to the nodal structure of the computers, computational hours were shared with the Coastal Engineering group at UDel. At times, finding available nodes to run model simulations was difficult and caused delays in data acquisition.

To compound the issues of nodal effects in high-powered computing, the Mills cluster suffered a catastrophic failure. Of the six hard disks comprising the cluster system, data can be preserved if two or fewer disks suffer failure. In the process of running and compiling this model, three hard disks were destroyed, this caused a catastrophic failure of the supercomputing capability at UDel and data along with model updates were lost. Recreating the model data was both difficult and time consuming.

THIS PAGE INTENTIONALLY LEFT BLANK

IV. EXPERIMENTAL APPROACH

A. INTRODUCTION

Measurements from the accompanying data report to CK02 are used to test NHWAVE model output for cases of refractive shoaling through a tank of varying width. Each simulation was done using monochromatic waves on a constant opposing tidal flux. A two-dimensional wave tank domain modeled after the CK02 tank experiment was created to simulate a river inlet. The goal was to see how well NHWAVE predicts wave-current dynamics in regions where wave-blocking occurs and compare results to those of CK02 in the hope of verifying the application of NHWAVE to wave blocking cases.

B. TEST TANK CONFIGURATION

The CK02 data set was acquired in a 30.0 m long recirculating wave flume at the Center for Applied Coastal Research at the University of Delaware. The width of the flume is 0.60 m wide with a constant depth of 0.50 m (Figure 6). The coordinate system is oriented so that the positive horizontal axis, x, is the direction of wave propagation, x=0 at the location of wave generation. The y-coordinate axis has an origin on the continuous sidewall (right side) and points toward the narrowed wall that was created to represent the inlet. The z-axis is positive upwards with z=0 at the still water level.

A false wall was implemented starting at x=12.4 m to gradually narrow the tank to 0.36 m by 15.2 m in the tank. The narrowing of the channel was designed to represent a tidal inlet where energy density and current velocity would increase in the narrow section of the tank. This design, coupled with a constant opposing current, was intended to block waves with periods up to 1.3 s in a 0.5 m depth. The depth-averaged current throughout the flume was increased through the narrow shoal region, but maintained relative depth uniformity. After 4.9 m of the narrow section, the tank width gradually widens at five degrees to the original dimensions negating flow separation at the transition.

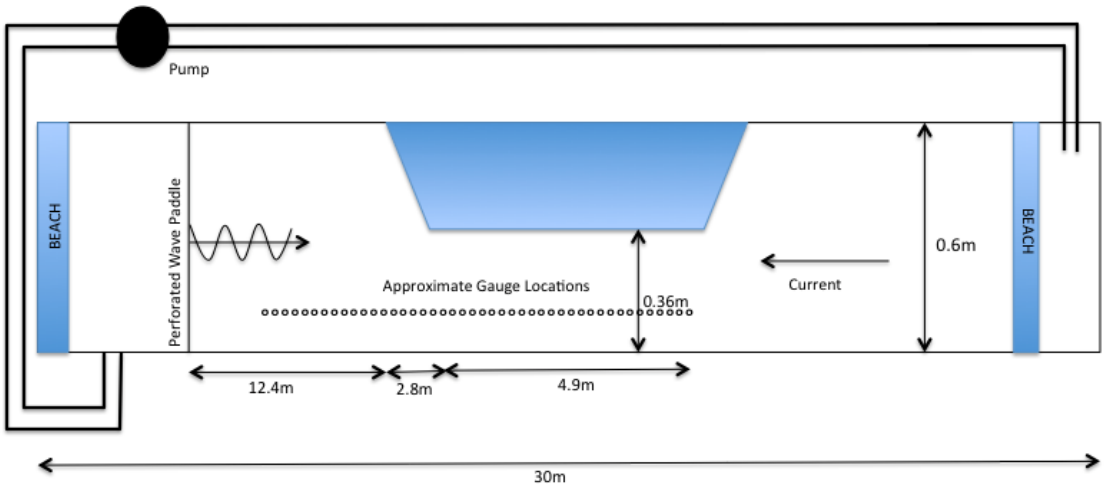

Figure 6. Schematic for Chawla and Kirby tank experiment (After Chawla and Kirby 2002). Not to Scale.

Waves were generated on the west side, (x=0). The current was created by drawing water from behind the perforated wave maker and pumping it to the opposite (Eastern) end of the tank. Care was taken to ensure there were no large-scale eddies. A complete description of the mechanics of the wave tank and the experimental method in the lab are found in Chawla and Kirby (1999).

For the CK02 data, capacitance wave gauges were used to measure the free surface elevation and Acoustic Doppler Velocimeters (ADVs) measured fluid velocities. In the model applications, free surface elevation and fluid velocities were calculated at approximately the same locations as the CK02 instruments (Figure 6).

C. MODEL SET-UP

1. Domain

NHWAVE was initialized with a domain that was altered from the original tank experiments to account for model boundary condition constraints. The bottom grid was produced in a Matlab environment to simulate a tank that measured 70 m X 0.6 m (Figure 7). By increasing the length of the tank, effects from the wave-maker were reduced. The coordinate axis are the same as in the CK02 experiment. The computational grid was configured with 0.025 m resolution in the x-direction and 0.05 m resolution in the y-

direction. The depth was set at 0.5 m and the model was run with five vertical layers. A false wall was initiated at 39.4 m increasing in width from the tank sidewall boundary to narrow the channel to 0.4 m at 42.2 m in the domain. The simulated inlet then extends for 10 m before expanding at the same ratio to the original with of the tank, see Figure 3. A time step of 0.1 seconds was used for computational efficiency while maintaining high enough temporal resolution. Output was computed at gauge locations closely resembling the locations in CK02.

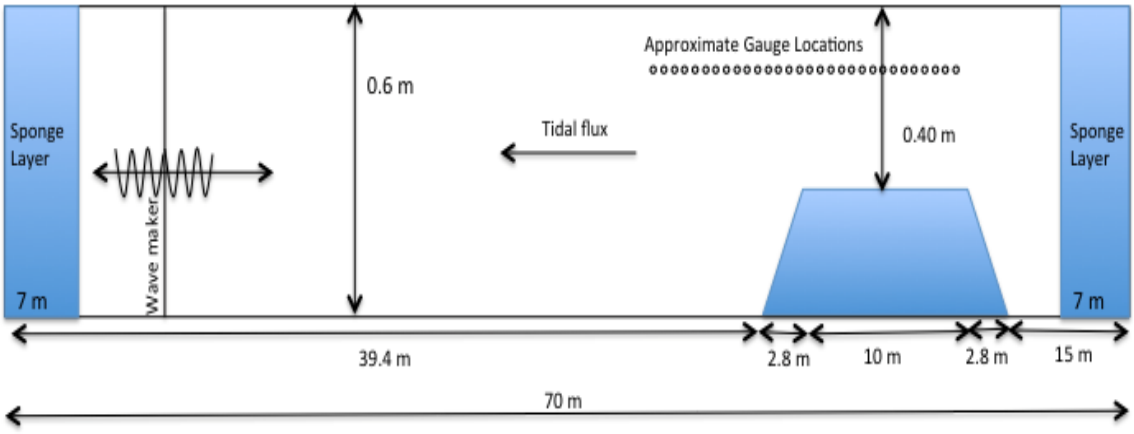

Figure 7. Schematic for NHWAVE model setup. Not to scale.

The artificial inlet wall was moved to many different locations in the tank and changed in dimension to attempt to replicate the currents and wave amplitudes present in CK02. The wall was defined with a no-slip boundary, which should have produced wave reflection and amplification in the tank when a current was not included. However, as the model results indicate, there was significant amplitude damping through the narrowed inlet (Figure 3). After increasing resolution to account for numerical dissipation, it was evident that the boundary conditions were not resolved for the model domain when a false wall was implemented.

Previous versions of NHWAVE were run in a domain replicating bathymetry present in the field. The boundaries in these cases are dissipative in that landmasses are absorb wave energy. This land masking allows the model to run with dissipation effects that would be expected in the environment. In the tank domain the depth of the tank was

0.5m. The false inlet wall was defined by a trapezoid that stood 1.0 m above the still water depth. This involves the model needing to account for wetting and drying of the boundary. The non-hydrostatic approximation allowed for pressure perturbations and vertical velocities to be introduced in the domain. In the tank model runs, the pressure field showed errors in the presence of dry points in the domain. This boundary issue will need to be resolved in the future development of the model.

2. Wave Maker

Waves were created by a linear wave maker located 15 m in the tank. Due to the simplicity of the wave-maker, model input was adjusted to replicate wave amplitude at the first gauge in the experimental data. In CK02 the initial conditions were defined at the first gauge location that varied between 4.6 m to 5.8 m before the narrowest part of the channel; the initial conditions in the model were defined at similar distances from the narrowed inlet but implemented to replicate CK02 experimental data.

3. Sponge Layers

Sponge layers 7 m thick were placed at each end. The sponge layers were made thick and with a low decay rate to allow waves and currents to reach the boundary with little reflection back into the tank from the east/west boundary. This tank set-up with appropriate sponge layers allows simulating a refraction only inlet where wave blocking occurs close to the narrow part of the "inlet."

4. Current Flow

The mean current was assumed uniform in the vertical and cross-shore, due to the no-slip boundary verified previously. The current was given by

$$U \equiv -\frac{Q}{bh} \tag{16}$$

where b is the width of the channel and Q is the volume flux prescribed as a tidal flux in the input boundary conditions. In this equation, boundary layer effects are ignored so that the value of Q was adjusted to 0.05 m^3/s to match the data. The measured and calculated horizontal current profile through the narrowing of the tank is presented in (Figure 8).

The profile agrees well with theory in the transition to the inlet and the faster laminar flow located there. There is an increase in the current speed just prior to the inlet opening back to the width of the channel. This jump could lead to inconsistencies in data at the inlet transition area. This deviation from the tank data is due to a pressure field imbalance at the inlet boundary to be explained in Chapter V.

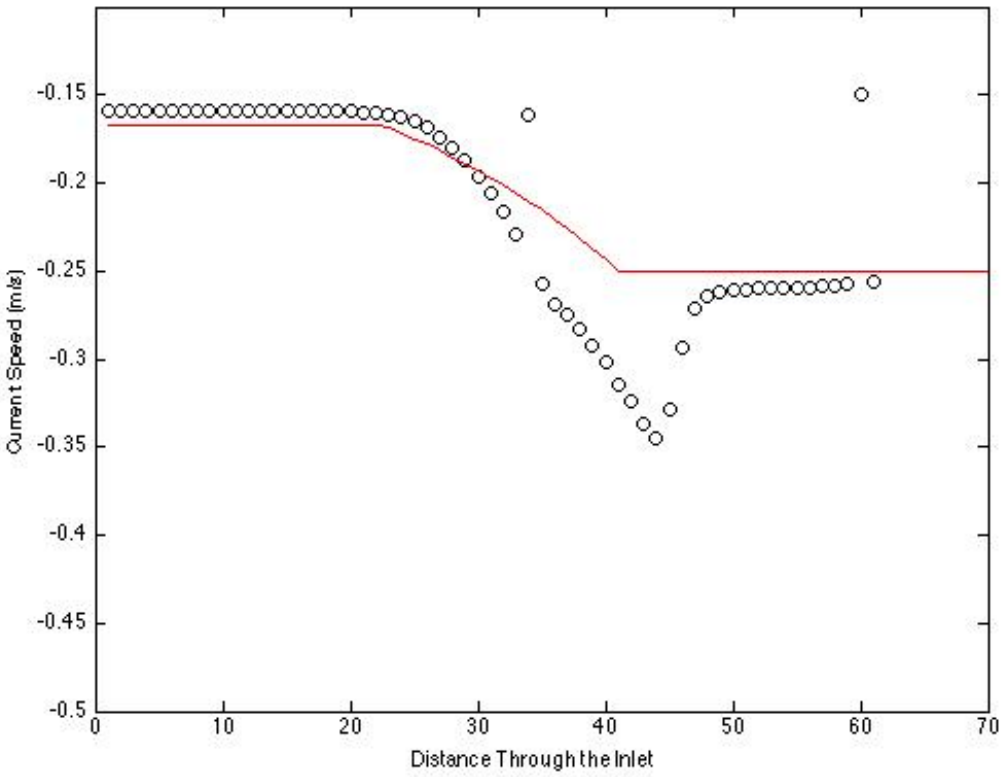

Figure 8. Horizontal current distribution through the narrowing of the inlet. (Model output circles (o), and theory solid line.)

As determined in the development of the model, vertical and cross-tank horizontal velocity mean profiles through 400 s in five different locations within the tank showed little variation, and thus the uniform assumption was valid. This allows for application of equations in a one-dimensional sense. Velocity profiles throughout the tank show relative depth uniformity with an average current of 0.2 m/s outside the inlet and 0.32 m/s

throughout the narrowed section (Figure 9). Decreasing the current from CK02 observations allowed a slower transition through the inlet and less instability in the model data.

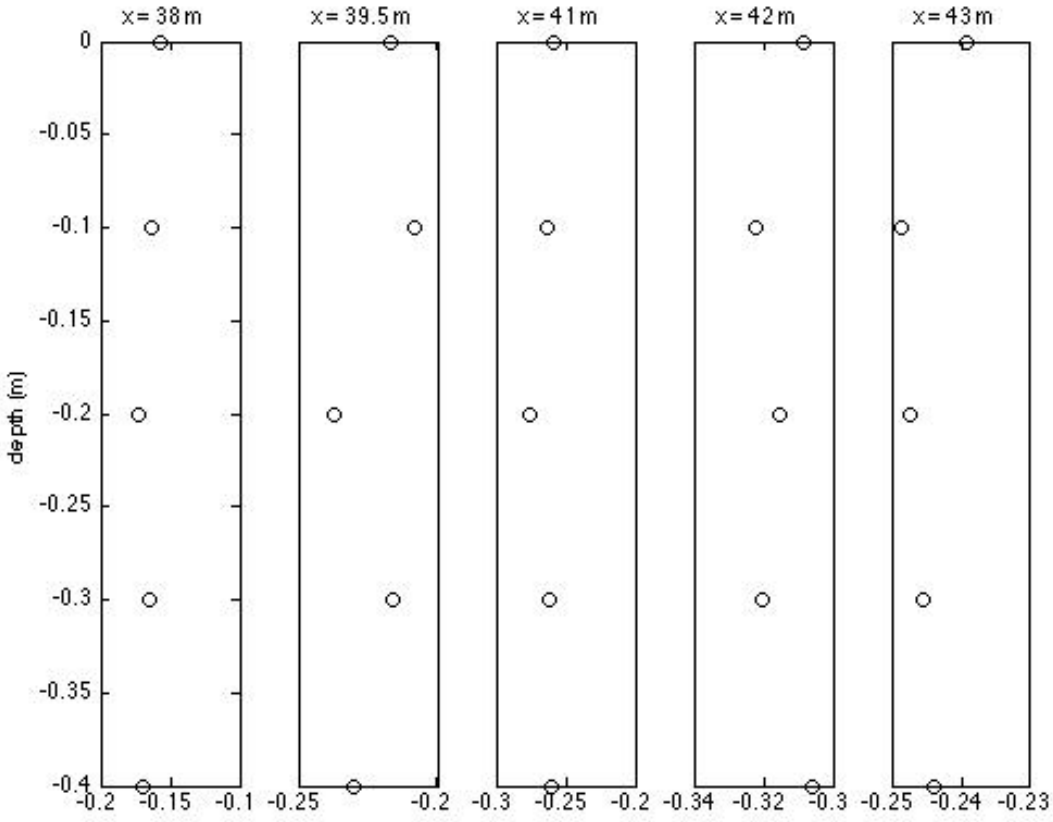

Figure 9. Vertical current distribution in five locations along the tank.

The current in the model tank showed inconsistencies through the narrowed inlet. Laminar flow was present in the wide area of the tank at both the east and west side just after the sponge layers. As the current flows over the narrowing section of the wall from the east, there is marked instability. Laminar flow is then re-established through the narrow section, this is where model conditions were measured from for data comparison (Figure 10). The surface current becomes faster than the current at the bottom of the tank. This creates a bore-like situation where one shouldn't be present and suggest that there is a boundary problem. The current then "jumps' before exiting the inlet. This could be the

cause for what appears to be wave blocking in the model data, however it is a function of problems with the pressure field around the false wall.

In examining the current only case the surface also shows shape change over the opening of the inlet (Figure 10). The inconsistencies over the eastern narrowing are present, as well as a dip in elevation at the opening of the inlet. Froude numbers in the narrowed inlet were 0.14 and decreased to 0.07 in the less constrained flow. These numbers do not indicate an approach to critical flow and therefore, super-critical flow should be excluded from consideration for the formation of a bore-like element. These inconsistencies in the data perpetuated more development of the numerical scheme for boundary conditions.

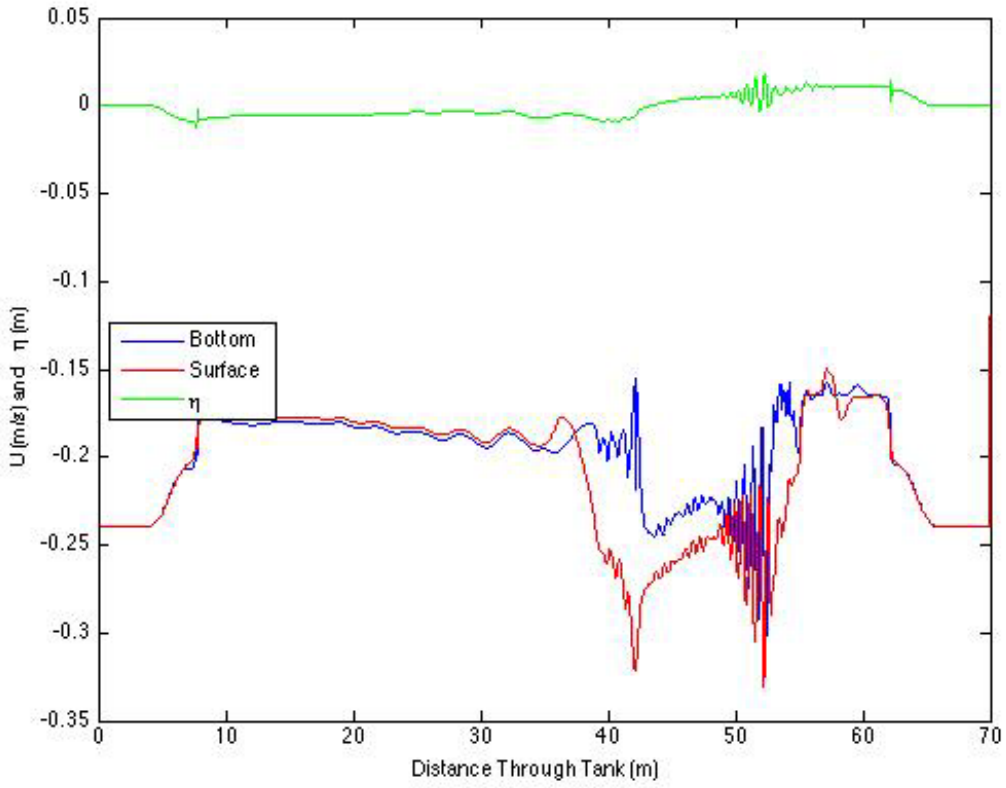

Figure 10. Surface elevation in the current only case (green).
Current profiles at surface (red), and at tank bottom (blue).

The wet/dry boundary issue also causes vertical velocities to appear with changes in the pressure field. The laminar flow should show no vertical accelerations whether in

the inlet or in the wide area of the tank. As the current flows through the inlet, the orbital velocities show vertical flow, an unexpected result in the model (Figure 11). This occurs both at the eastern side of the inlet, where flow is restricted, and also at the opening of the inlet to dissipative laminar flow. This result is shown through all layers of the current flow.

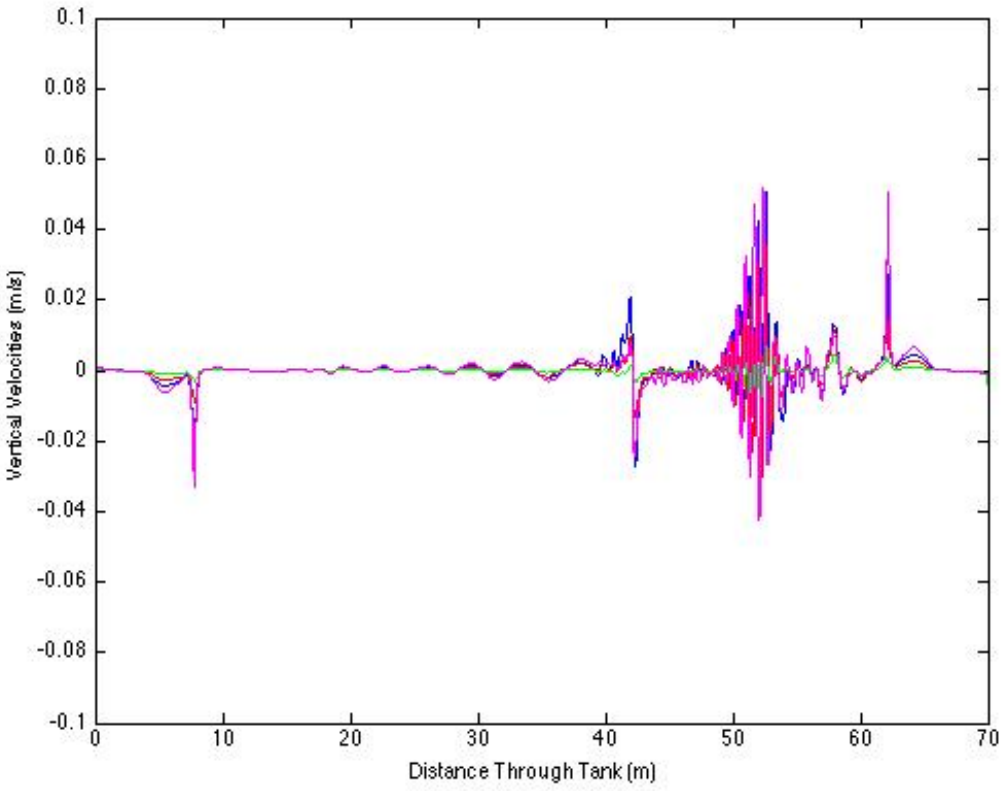

Figure 11. Vertical velocity instabilities in the current through the inlet. Multiple colors indicate multiple layers from magenta at the surface, to blue, red, and then green at the bottom.

V. WAVE BLOCKING TESTS

A. INTRODUCTION

The extensive data that were collected for CK02 is compared to NHWAVE model data. In the CK02 test cases, wave periods ranged from 1.2 to 1.6 s. The waves created in the experiment were intermediate-depth water waves with *kh* values outside the narrow channel ranging from 1.35 to 2.4, as determined using a Doppler-shifted linear dispersion relation (Chawla and Kirby 2002). The *kh* values increase inside the narrow channel where currents are stronger. By narrowing the channel in the experiment, waves were shown to shoal with or without an opposing current. Conditions meant to replicate this data were explored in the model. The results of the NHWAVE model runs were not accurate in predicting the wave blocking and breaking conditions as seen in CK02. Constraints in modeling in a tank domain have been found to cause instabilities and false results in the model.

Each case for monochromatic waves was divided into two parts, small amplitude where waves should reflect from the blocking point without breaking, and larger amplitude waves where breaking occurs. The study of the amplitude envelope through the blocking region as well as the energy transformation and dissipation through the region was accomplished by implementing a range of wave heights with different wave periods in the experimental and model initial conditions. Each model run was conducted to attempt to mimic the wave blocking results in CK02, however, the model was unsuccessful in resolving the wave components with the current numerical scheme.

B. THEORETICAL EXPECTATIONS AND CK02 RESULTS

1. Monochromatic Small Amplitude Reflected and Blocked Wave Tests

In monochromatic, small amplitude tests, wave energy cannot propagate beyond the blocking point and no energy is lost due to breaking at or before the blocking point; therefore, there is wave reflection. From previous studies, these reflected waves are unique in that the phase speed of the waves continues to move against the current, however, the group velocity moves with the current with the wave energy (Chawla 1999).

For the monochromatic wave blocking tests, three different periods were used with increasing wave amplitude to study the wave amplitude dynamics through the blocking region and were compared to CK02 data.

In linear wave theory, if there is no wave breaking in the domain and the wave amplitude and steepness is small enough that waves will be reflected from the blocking point with a different wave number. The amplitude envelope of these waves through the blocking point resembles an Airy function (Peregrine 1976). CK02 data verified this results for small amplitude monochromatic wave tests.

In the experimental data, the change in the amplitude envelope is clearly visible in the smallest wave cases. The test cases presented here are for the 1.2 s period. Wave height measurements are made in relation to the blocking point with x=0 indicating the narrowest part of the test tank. As the amplitude increased and approached the breaking steepness criteria as defined by Miche (1951), the node and antinodal resemblance to an Airy function is diminished (Figure 12). Non-linear effects change the steepness of the wave reflection response, which can be seen by the increasing deviation in the primary wave's peak and slope as the amplitude increases.

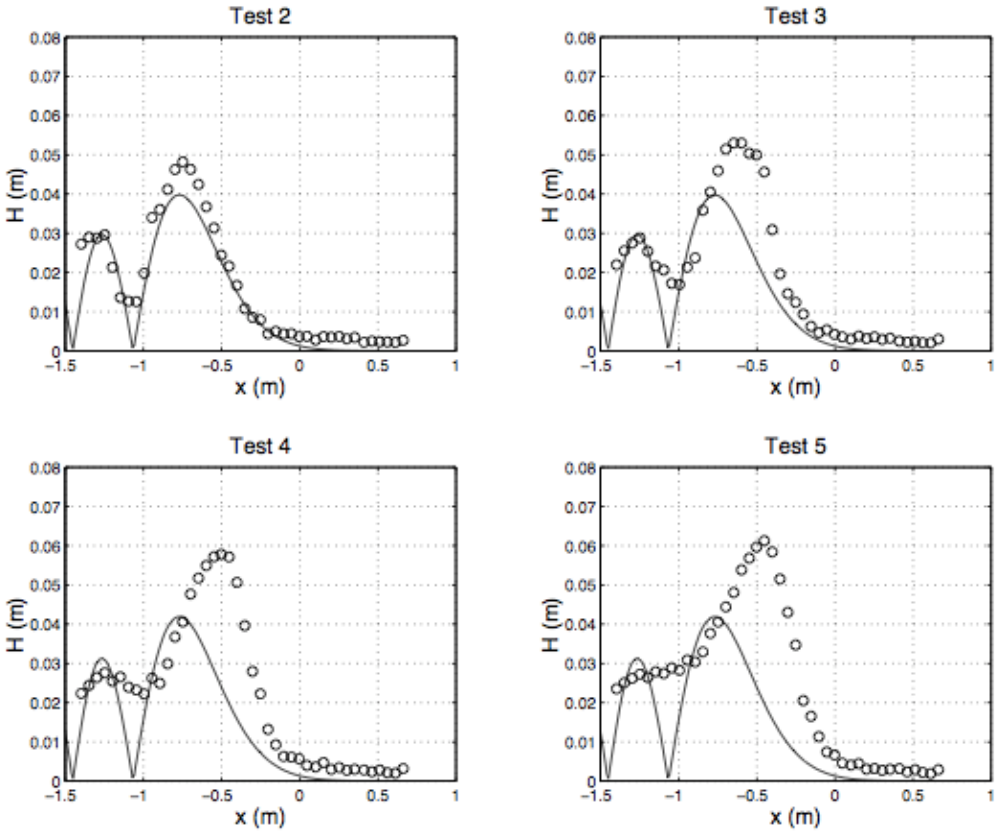

Figure 12. Comparison between measured CK02 data and Airy function for small amplitude monochromatic waves. Amplitude increases from 1.3 cm in test 2 to 1.6 cm in test 5 (From Chawla 1999).

2. Monochromatic Breaking Wave Tests

In CK02, each test was conducted similar to the small amplitude conditions in that multiple amplitudes were examined for different wave periods. A simple numerical model was created to study the wave breaking in this tank configuration. The bore model using third order Stokes relations were able to handle the location of the breaking and blocking of the wave field well. However, it was insufficient to predict the side-band instabilities and energy shifts seen in the data. The hope was that NHWAVE would be able to predict these.

a. Energy Spectra

One of the main findings in CK02 was the frequency downshift in the energy spectrum of monochromatic breaking waves. This shift is a result of the nonlinear side band instabilities. These are dependent on the frequency and amplitude of the wave field and effect the wave propagation greatly (Benjamin and Feir 1967). As the waves become steeper on the opposing currents and approach the blocking point, the group velocity approaches zero and wave energy travels very slowly (Lai et al. 1989). Therefore energy can be shifted to a lower sideband, which requires a higher blocking current. This will allow the wave components in this lower side band to travel into the narrow inlet while the higher frequency waves are blocked, and further increase the energy in the lower side-band as a function of distance through the inlet. The result is that the primary wave component has reached its blocking condition, while the lower sideband propagates through the channel.

The spectra from CK02 wave breaking conditions show the frequency shift to lower sidebands (Figure 13). For probe locations around the blocking point, indicated in CK02 as x=0, the primary (P), upper (U), and lower (L) sidebands show modification of the frequency spectra. Energy in the upper and primary sideband decreases with progression into the inlet while there is marked lower sideband growth. This supports the theory of higher frequency energy being blocked while lower sideband waves are allowed to propagate through the inlet. The non-linear aspect of the lower sideband growth was not predicted by the simplified model used in CK02.

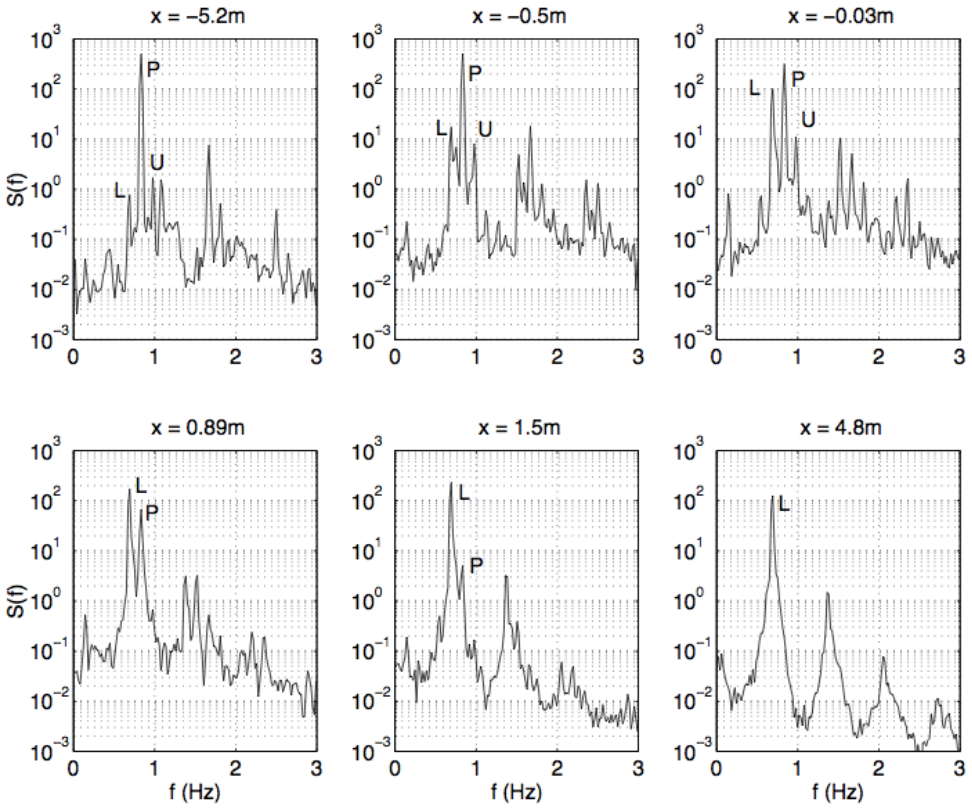

Figure 13. Frequency spectra for a wave breaking test from CK02 with period=1.26 s and amplitude=0.126m (L=lower side band, P=primary side band, U=upper sideband) (From Chawla 1999).

C. NHWAVE PRELIMINARY RESULTS

Model output of surface height, η, and velocities in the u, v, and w directions were output in the model over the domain and through the five vertical layers in the simulated tank. Comparison tests for CK02 data were unsuccessful. However, recent developments have made some wave blocking cases in a tank with a narrowed inlet possible.

1. NHWAVE Performance

Each case of monochromatic wave blocking and wave breaking was initially attempted in NHWAVE for comparison to data from CK02. Wave height distributions through the blocking point show vast differences from theory and experimental data due to the unresolved boundary conditions. In some cases NHWAVE showed a wave height distribution that appeared to have wave blocking for the range of small amplitude waves

tested. In these cases, the reflected wave was not apparent in any of the measurements. Coupled with the wave dissipation caused by the pressure field inaccuracy through the inlet, these results do not verify the model.

Larger amplitude waves cases were also examined using the wave height distribution to determine if the waves broke at, or just prior to, the blocking point of the inlet. In those tests where a steep drop in amplitude around the blocking point indicated that waves were breaking, wave period and spectra were examined and compared to CK02 data. The model shows significant deviation from the expected wave height distribution and energy spectra through the blocking point and into the inlet.

2. Recent Model Developments

Preliminary results from a new iteration of NHWAVE are promising for wave blocking cases. For these cases a new tank domain that measured 35 m long by 0.6 m wide was created (Figure 14). The tank has a simulated inlet 7.5 m long centered at 20 m in the tank. The inlet narrowed the overall width of the tank to 0.3 m. For the new test cases, resolution was 0.025 in x and 0.05 in y. This was shown previously to negate numerical dissipation issues from low resolution test runs. Sponge layers were 5 m thick on either end of the tank and had the same decay coefficients and low pass filter as used previously.

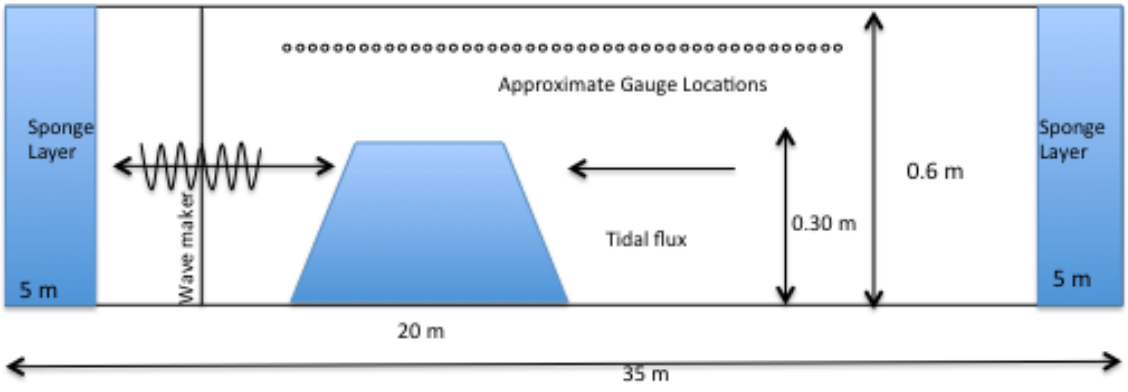

Figure 14. Simplified test tank for preliminary model results. (Not to Scale)

By implementing a new Poisson solver for the issue of the land masking and the wet/dry boundary, the pressure field inconsistencies have been resolved. In a simple tank with an inlet wall halfway down the "tank" wave amplitude increases through the inlet as would be expected before decreasing due to diffraction as the tank widens again (Figure 15).

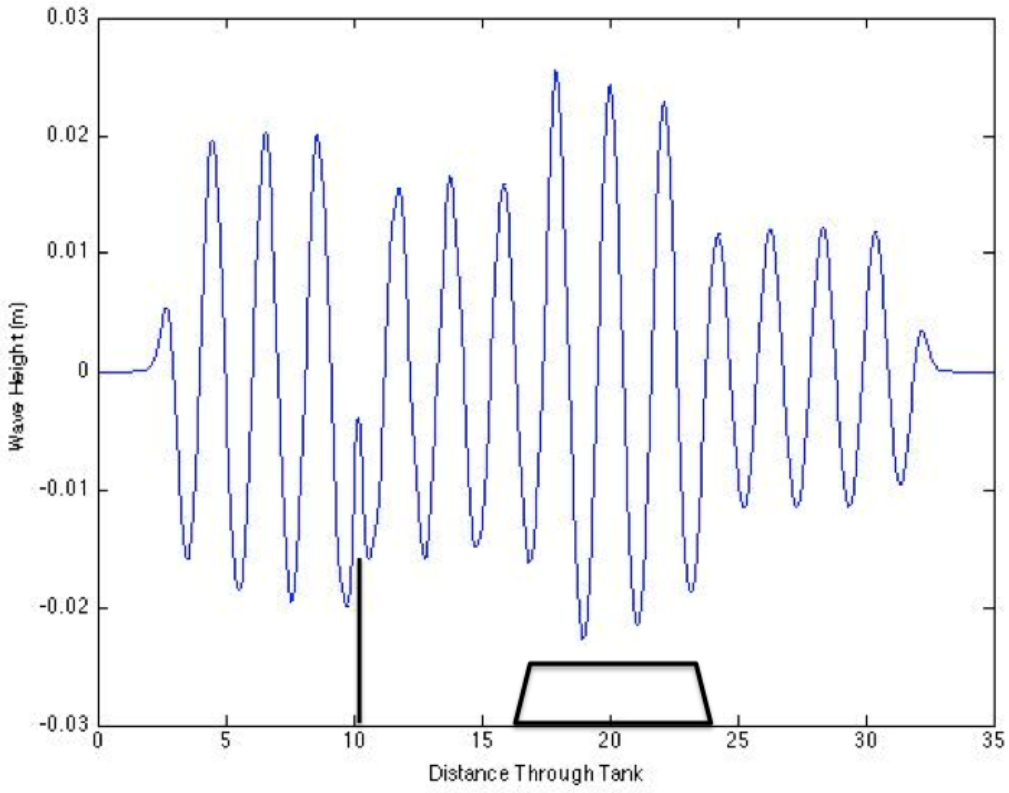

Figure 15. Wave height in simplified tank. Inlet wall location is indicated by the trapezoid, the wave maker is located at the vertical line.

a. Preliminary Wave Blocking Results

For small amplitude waves, blocking conditions were met in the NHWAVE data. Waves shoaled slightly as they approached the wall and decrease in amplitude due to the opposing current at the end of the inlet. As the current is increased from 0.28 m/s (Figure 16a) in the tank to 0.35 m/s (Figure 16b), the blocking criteria is reached for the test wave of period 1.3 s and initial amplitude of 0.09 m. With increased

current, the shoaling is more pronounced and the wave steepness is greater. This causes the wave to break as seen in the rapid decrease in wave amplitude. Therefore, for small amplitude waves, the effect of increased current through the inlet shows blocking criteria being met for the given wave parameters.

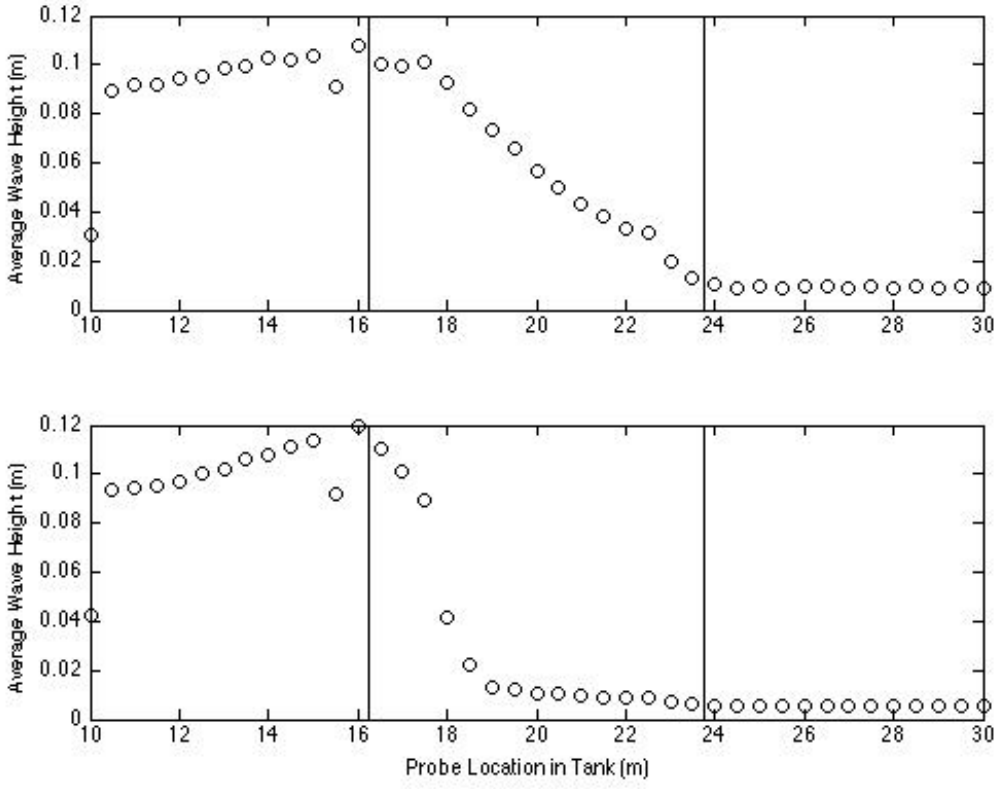

Figure 16. Small amplitude wave blocking and reflection. Solid lines indicate the boundaries of the inlet wall. a) Opposing current=0.28 m/s b) Opposing current=0.35 m/s. Vertical lines indicate the boundaries of the inlet wall.

Similarly, in a large amplitude cases, with a period of 1.3 s and amplitude of 30 cm, waves show an increase in amplitude just prior to the narrowing of the inlet and breaking at the narrowest section for the larger current. Again implementing an opposing current of 0.28m/s caused the waves to shoal against an opposing current, but not break (Figure 17a). With increased speed, 0.35 m/s, the waves broke upon entering the narrowed inlet (Figure 17b). This is consistent with the theory presented here as well as the results from CK02.

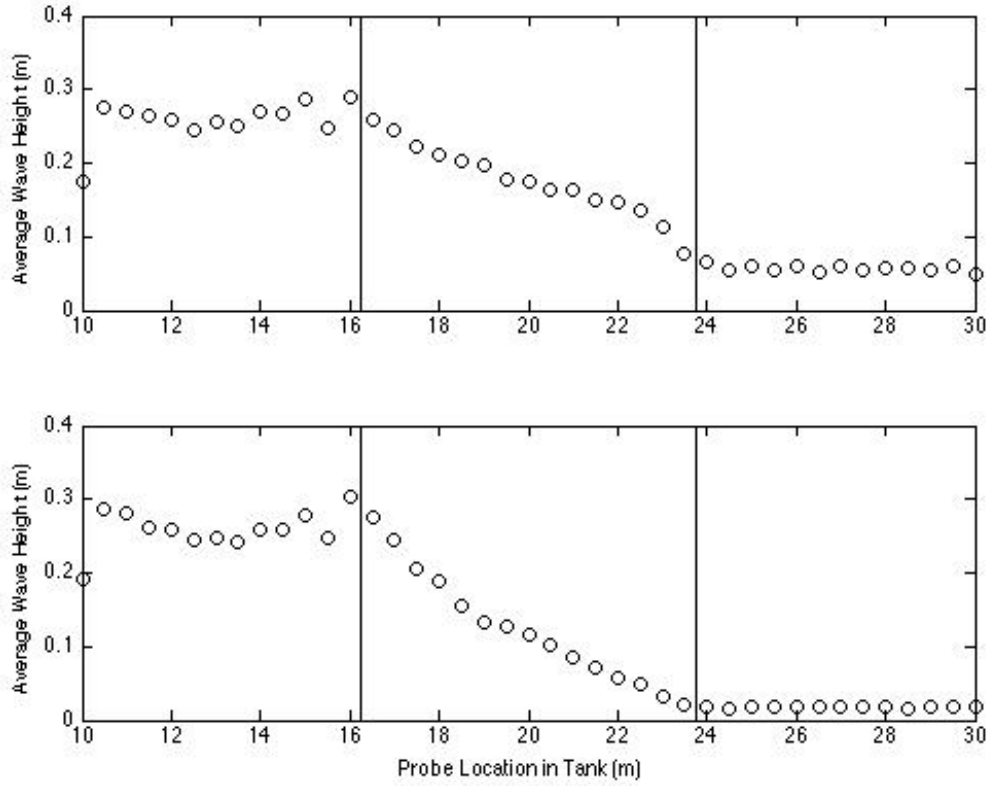

Figure 17. Wave height distribution for a large amplitude wave breaking case. Vertical lines indicate the boundaries of the inlet wall.

Time series analysis for energy spectra were not available due to the shortened data record for the simplified cases. Further statistical analysis is needed to determine if NHWAVE can be validated in comparison to CK02 for wave blocking cases.

3. Extension to Random Wave Spectra

The validation attempts for NHWAVE were conducted with monochromatic waves only. One of the benefits of the CK02 data was examining the changes in the frequency spectra through the breaking and blocking region with wave groups. Extension to more realistic spectra for a better understanding of the environment is needed in NHWAVE. Currently, efforts to include implementing Jonswap spectra are being attempted. However, results are not reliable at this time.

THIS PAGE INTENTIONALLY LEFT BLANK

VI. CONCLUSIONS

The complex dynamics of wave blocking are difficult to model. Current wave averaged models under predict the non-linear processes that occur within short distances of a wave blocking location. Two models were recently developed to model fully dispersive wave processes and were explored for their use in river inlets where blocking conditions exist. The testing of both SWASH and NHWAVE proved boundary conditions involved in a tank setting necessitated modifications to the model code and numerical processes therein. Multiple iterations of NHWAVE were developed for this application and resolution of boundary condition issues proved difficult, but in the end, successful.

Model testing using a series of monochromatic wave cases on opposing blocking currents was conducted with NHWAVE. Two classifications of tests were presented, those with small amplitudes where waves were reflected, and those with higher amplitudes that demonstrated wave breaking prior to the blocking point. These tests were compared to data from CK02.

Data from CK02 were able to show monochromatic wave blocking and wave breaking on opposing currents. Waves that were reflected at the blocking point showed a distribution close to an Airy function for small amplitude waves. This is a close approximation to linear theory that breaks down as wave amplitude increases. In larger amplitude wave breaking cases non-linear effects are increased and seen in the energy spectra. The changes in the energy spectra indicate unstable sideband growth that is difficult to model. NHWAVE in its current state is unable to replicate the CK02 tank experiment due to boundary conditions that cause amplitude dissipation through the narrowing of the inlet.

Future work on random wave field input to NHWAVE as a Jonswap spectrum is needed. At the moment, the model is unable to handle a random wave field or wave group that would be more pertinent to field data.

NHWAVE, while still under development, allows us to explore many conditions that are not always possible with field or lab measurements and shows promise as an

accurate predictor of wave-current interactions and wave blocking. In comparison to CK02 lab data, there are shortfalls in the numerics of the model that are greatly affected by boundary conditions. Preliminary results with improved equations for boundary conditions show promise for future implementation of the model. More development will lead to improved understanding of the wave blocking conditions in river inlets. The future implementation of a non-hydrostatic model for the intense kinematic conditions in wave-current interactions and wave blocking scenarios will be a valuable addition to our knowledge base of these turbulent areas.

LIST OF REFERENCES

Benjamin, T. B., and Feir, J.E., 1967: The disintegration of wave trains on deep water. Part 1. Theory, *Journal of Fluid Mechanics,* **27**, 417–430.

Bretherton, F. P., and C. J. R. Garrett, 1969: Wavetrains in inhomogeneous moving media, *Proc. R. Soc. London, Ser. A.,* **302,** 529–554.

Chawla, A., and T. J. Kirby, 1998: Experimental study of wave breaking and blocking on opposing currents, *Proc. Int. Conf Coastal Eng.,* **26***,* 759–772.

Chawla, A., 1999: An experimental study on the dynamics of wave blocking and breaking on opposing currents. Ph.D. dissertation, University of Delaware, 151 pp.

Chawla, A., and T. J. Kirby, 1999: Waves on opposing currents: Data report, *Tech. Rep CACR-99–03,* Cent. For Appl. Coastal Res., Univ. of Delaware, Newark, Del.

Chawla, A., and T. J. Kirby, 2002: Wave breaking at blocking points, *J. Geophys. Res.,* **107***,* 1–19.

Heitner, K. L., and G. W. Housner,1970: Numerical modeling for tsunami runup, *J. Wtrwy.,Port, Coast., and Oc. Engrg.,* ASCE, New York, 217–233.

Jonsson, I. G., 1990: Wave-current interactions, *The Sea, Ocean Eng. Science,* **9A**, 65–120.

Kennedy, A. B., Q. Chen, J. Kirby, and R. A. Dalrymple, 2000: Boussinesq modeling of wave transformation, breaking, and runup, *J. Wtrwy.,Port, Coast., and Oc. Engrg.,* **126,** 39–47.

Kramer, S. C., and G. A. Stelling, 2008: A conservative unstructured scheme for rapidly varied flows, *Int. J. Numer. Meth. Fluids*, **58***,* 183–212.

Lai, R. J., S. R. Long, and Huang, N. E., 1989: Laboratory studies of wave-current interaction: Kinematics of the strong interaction*, J. Geophys. Res.,* **94,** 201–16.

Ma, G., Shi, F., and Kirby, J. T., 2012: Shock-capturing non-hydrostatic model for fully dispersive surface wave processes, *Ocean Modeling,* **43–44***,* 22–35.

Miche, R., 1951: Le Pouvoir reflechissant des ouvrages maritime exposes a l'action de la houle, *Annales Ponts et Chausses*, **121**, 285–319.

Peregrine, D. H., 1976: Interaction of water waves and currents, *Adv. Appl. Mech.,* **16**, 9–117.

Phillips, N. A., 1957: A coordinate system having some special advantages for numerical forecasting, *J. Meteor.*, **14***,* 184–185.

Ris, R. C. and L. H. Holthuijsen, 1996: Spectral modeling of current induced wave-blocking. 25th *Int. Conf. Coast. Engng.,* 1246–1254.

Shi, F., Ma, G., Kirby, J. T., and Hsu, T. J. T., 2012: Application of a TVD solver in a suite of coastal engineering models, *Coastal Engineering Proceedings*, *1*(33), currents-31.

Smith, R., 1975: Relection of short gravity waves on a non-uniform current, *Math. Proc. Camb. Phil. Soc.,* **78**, 517–525.

Stelling, G., and M. Zijlema, 2003: An accurate and efficient finite-differencing algorithm for non-hydrostatic free surface flow with application to wave propagation, *Int. J. Numer. Meth. Fluids* **43***,* 1–23.

Tao, J., 1983: Computation of wave run-up and wave breaking, *Internal Rep.,* Danish Hydrolics Institute, Horsholm, Denmark.

Tehranirad, B., J. T. Kirby, F. Ma, and F. Shi, 2012: Tsunami benchmark results for non-hydrostatic wave model NHWAVE, Version 1.0*, Research Report No. CARC-12–03*, Cent. For Appl. Coastal Res., Univ. of Delaware, Newark, Del.

Thornton, E. B., and R. T. Guza, 1983: Transformation of wave height distribution, *J. Geophys. Res.,* **88***,* 5925–5938.

Zelt, J. A., 1991: The run-up of nonbreaking and breaking solitary waves, *Coastal Engrg*., **15**, 205–246.

Zijlema, M., G. Stelling, and P. Smit, 2011: SWASH: An operational public domain code for simulating wave fields and rapidly varied flows in coastal waters, *Coast. Engng*. **58**, 992–1012.

Zijlema, M., and G. Stelling, 2008: Efficient computation of surf zone waves using the nonlinear shallow water eqations with non-hydrostatic pressure, *Coast. Engng*. **55**, 780–790.

INITIAL DISTRIBUTION LIST

1. Defense Technical Information Center
   Ft. Belvoir, Virginia

2. Dudley Knox Library
   Naval Postgraduate School
   Monterey, California